Chain Configurations in Lamellar Semicrystalline Polymer Interphases

J. A. Marqusee*

Polymers Division, National Bureau of Standards, Gaithersburg, Maryland 20899

Ken A. Dill

Departments of Pharmaceutical Chemistry and Pharmacy, University of California, San Francisco, California 94143. *Received April 4, 1986*

ABSTRACT: A mean-field lattice theory is developed to describe the configurations of long-chain molecules at the crystal/amorphous interface in semicrystalline polymers. Chains are assumed to satisfy continuity and space-filling requirements. The theory permits systematic levels of approximation for correlations among neighboring bonds along the chains subject to the interfacial constraints. We consider the two lowest levels of approximation here: (i) single bonds (two segments) or (ii) bond pairs (three segments). Both models predict that approximately 73% of the chains which emerge from the crystal reenter at sites which are immediately adjacent and that the interfacial region should therefore be small, provided the chains are freely flexible. The models predict that the ratio of chain loops to ties in the amorphous region is smaller, and the mean lengths are greater, than predicted by random walk models.

Introduction

The thermal and mechanical properties of semicrystalline polymeric materials depend on the molecular organization of the chain molecules which comprise them. Long-chain polymers cooled from the melt form lamellar crystals which are generally 100–500 Å thick and are separated by amorphous regions with dimensions of 50–200 Å.[1] Inasmuch as the lengths of the constituent chains are usually much greater than these dimensions, each chain may traverse crystalline and amorphous regions many times.

The details of the molecular organization in the crystal/amorphous interfacial regions are not yet well understood. Several years ago, Flory argued that a significant fraction of the chains which exit the crystallite must reenter it, for otherwise the chains would overfill the volume available to them in the amorphous region.[2] An issue which has remained unresolved since that time is whether each chain reenters at a site adjacent to that form which it exits the crystal or whether it reenters more randomly relative to the site from which it exits the crystal.[3,4]

Recently, several theoretical models have been introduced to predict the chain conformations in the semicrystalline interphase;[5–9] one of the principal properties they have attempted to predict is that of adjacency of reentry. Two of these models take into account the interfacial constraints[8,9] and both of them predict that the interface is not perfectly sharp; instead, there is a gradient of disorder along an axis parallel to the crystalline chains toward the amorphous bulk. The details of these models differ significantly, however. For example, for freely flexible chains, the only situation for which the two models can be compared, one of them predicts that adjacent reentry is dominant,[8] while the other predicts that random reentry is dominant.[9]

Here we present a different treatment for the chain conformations in the semicrystalline interphase, one which also provides a basis for resolving the discrepancy between the earlier models. Our approach permits systematic levels of approximation for correlations among neighboring bonds, two levels of which we consider explicitly here. Although the model can be readily extended to account for internal chain stiffness, the present work treats only freely flexible chains.

Model

We model two opposing crystal interfaces and the intervening amorphous zone of a lamellar semicrystalline polymer by a simple lattice similar to those previously used.[7–9] The crystalline region is assumed to be devoid of defects and is not explicitly represented. Its presence is accounted for by suitable boundary conditions on the chain configurations. The lattice is divided into a set of layers enumerated by the index l. They are parallel to the two crystal interfaces and perpendicular to the chain axis in the crystal. Each site in a layer is singly connected to one site in each neighboring layer and has $(z - 2)$ neighboring sites within the layer. All the results given below are for a cubic lattice with $z = 6$. Modification for other lattices is straightforward. The perfect crystal terminates at $l = 0$ where the chain configurations may include lateral steps. The second crystalline lamella begins at $l = M + 1$, beyond which the chains are perfectly crystalline (see Figure 1).

The polymer chains are modeled as walks of linearly connected segments, each of which occupies a single site. Chains emanate from one of the crystals ($l < 0$ or $l > M + 1$) and may either take a lateral step and form a tight fold and immediately reenter the crystal at an adjacent site or enter the amorphous region. Once in the amorphous region either the chain may form an amorphous loop by eventually returning to the crystalline face it emerged from or it may traverse the amorphous zone and form a tie molecule between the two crystalline lamellae. The total semicrystalline sample is composed of N_p polymer chains, each n segments long. The entire system may be considered to consist of repeats of the crystal/interphase/amorphous units described above. We characterize a particular set of chain configurations by the sequence $\mathbf{R} = \{\mathbf{r}_1,...,\mathbf{r}_k,...\}$, where $\mathbf{r}_k$ is the location of the lattice site which contains the kth segment.

The chain configurations are determined by maximizing the chain configurational entropy subject to the condition that the crystal is at the two boundaries ($l = -1$ and $M + 2$). The chains are treated as freely flexible, constrained only by their connectivity and the requirement that the lattice is completely filled with all sites singly occupied.

Configurational Entropy

The conformational entropy of the chains in the interphase is different from that of amorphous chains in the

0024-9297/86/2219-2420$01.50/0

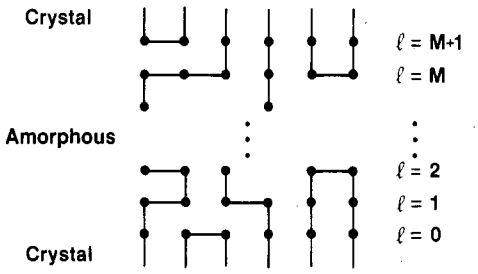

Figure 1. Schematic cross-sectional view of the amorphous region in a lamellar semicrystalline polymer. The crystalline regions before $l = 0$ and $l = M + 1$ consist of straight parallel chains.

bulk. The chains are more ordered as they emerge from the crystal. Below we construct an expression for the chain configurational entropy in terms of the local chain statistics. From the entropy the most probable configurational statistics can be determined and the type of configurations at the interface explored.

The entropy is

$$S = -k_B \sum_{\mathbf{R}} P(\mathbf{R}) \cdot \ln P(\mathbf{R}) - k_B \ln (\omega) \tag{1}$$

where k_B is Boltzmann's constant and

$$\omega = 2^{N_p} N_p! \tag{2}$$

which accounts for the indistinguishability of the molecules and their respective ends. $P(\mathbf{R})$ is the probability of a set of configurations $\mathbf{R}$. It is equal to zero if any site is not singly occupied (excluded volume constraint).

Following Helfand, we rewrite the probability as[10,11]

$$P(\mathbf{R}) = P_0(\mathbf{R}) \cdot \Lambda(\mathbf{R}) / \Psi \tag{3}$$

where $P_0(\mathbf{R})$ is not subject to the excluded volume restriction which is accounted for by Λ. $\Lambda(\mathbf{R})$ is zero if $\mathbf{R}$ includes any multiply-occupied sites and one otherwise. The factor Ψ normalizes the distribution and is given by

$$\Psi = \sum_{\mathbf{R}} P_0(\mathbf{R}) \cdot \Lambda(\mathbf{R}) \tag{4}$$

It is the fraction of all states which have no overlapping molecules. For chains in the amorphous region, it can be estimated by the Flory–Huggins approximation. Substituting eq 3 into the expression for the entropy yields

$$S = -\frac{k_B}{\Psi} \sum_{\mathbf{R}} P_0(\mathbf{R}) \Lambda(\mathbf{R}) \cdot \ln P_0(\mathbf{R}) - k_B \ln (\omega/\Psi) \tag{5}$$

We make the mean-field approximation that the sum restricted by $\Lambda(\mathbf{R})$ may be replaced by the unrestricted sum weighted by the fraction of allowed configurations. Thus[10,11]

$$\sum_{\mathbf{R}} P_0(\mathbf{R}) \Lambda(\mathbf{R}) \cdot \ln P_0(\mathbf{R}) = \Psi \sum_{\mathbf{R}} P_0(\mathbf{R}) \cdot \ln P_0(\mathbf{R}) \tag{6}$$

and the entropy is

$$S = -k_B \sum_{\mathbf{R}} P_0(\mathbf{R}) \cdot \ln P_0(\mathbf{R}) - k_B \ln (\omega/\Psi) \tag{7}$$

Consider the sequence of segments that comprise a chain configuration $\mathbf{R}$. The probability for the configuration is a product of conditional probabilities along the chain, $p(\mathbf{r}_{k+1}|\mathbf{R}_k)$

$$P_0(\mathbf{R}) = \prod_{k=0}^{n-1} p(\mathbf{r}_{k+1}|\mathbf{R}_k) \tag{8}$$

where $\mathbf{R}_k$ is the configuration of the previous k segments.

We treat the chain configurations by two different levels of approximation. The simplest is a Markovian approximation. We assume that the conditional probabilities depend only on the location of the previous segment along the chain

$$p(\mathbf{r}_{k+1}|\mathbf{R}_k) = p(\mathbf{r}_{k+1}|\mathbf{r}_k) \tag{9}$$

where $p(\mathbf{r}_{k+1}|\mathbf{r}_k)$ is the probability that the $(k + 1)$th segment is at $\mathbf{r}_{k+1}$ given that the kth segment is at $\mathbf{r}_k$. In this approximation, the conditional probability depends only on the location in the lattice and not on the position along the chain. This is justified for long chains for which the chain ends are an insignificant fraction of all chain segments.

The entropy can be simplified by using this one-segment approximation to the conditional probability. Substituting eq 9 and 8 into eq 7 yields

$$S^{(1)} = -k_B \sum_{k=1}^{n-1} \sum_{\mathbf{R}} P_0(\mathbf{R}) \cdot \ln p(\mathbf{r}_{k+1}|\mathbf{r}_k) - k_B \ln (\omega/\Psi) \tag{10}$$

where we have neglected terms due to end effects [$-k_B \ln p(\mathbf{r}_1)$] and the superscript (1) denotes the level of approximation. Summing over all $\mathbf{R}$ except $\mathbf{r}_{k+1},\mathbf{r}_k$ leads to[12]

$$\sum_{\mathbf{R}} P_0(\mathbf{R}) \cdot \ln p(\mathbf{r}_{k+1}|\mathbf{r}_k) = \sum_{\mathbf{r}_k,\mathbf{r}_{k+1}} \ln p(\mathbf{r}_{k+1}|\mathbf{r}_k) \sum_{\substack{\mathbf{R} \\ (\text{excl } \mathbf{r}_k,\mathbf{r}_{k+1})}} P_0(\mathbf{R}) \tag{11}$$

Since

$$\sum_{\substack{\mathbf{R} \\ (\text{excl } \mathbf{r}_{k+1},\mathbf{r}_k)}} P_0(\mathbf{R}) = p(\mathbf{r}_{k+1},\mathbf{r}_k) = p(\mathbf{r}_{k+1}|\mathbf{r}_k) p(\mathbf{r}_k) \tag{12}$$

then

$$S^{(1)} = -k_B \sum_k \sum_{\mathbf{r}_k,\mathbf{r}_{k+1}} p(\mathbf{r}_{k+1}|\mathbf{r}_k) p(\mathbf{r}_k) \cdot \ln p(\mathbf{r}_{k+1}|\mathbf{r}_k) - k_B \ln (\omega/\Psi) \tag{13}$$

where the two-segment joint probability, $p(\mathbf{r}_{k+1},\mathbf{r}_k)$, is the product of the conditional probability, $p(\mathbf{r}_{k+1}|\mathbf{r}_k)$, and the single-segment probability, $p(\mathbf{r}_k)$. Under the assumption that there is equal likelihood that segment k occupies any position in space

$$p(\mathbf{r}_k) = 1/V \tag{14}$$

where V is the volume of the system in lattice units. Also, since all sets of segments k and $k + 1$ are equivalent

$$S^{(1)} = -k_B \sum_{\mathbf{r}_{k+1},\mathbf{r}_k} p(\mathbf{r}_{k+1}|\mathbf{r}_k) \cdot \ln p(\mathbf{r}_{k+1}|\mathbf{r}_k) - k_B \ln (\omega/\Psi) \tag{15}$$

where the number of segments is equal to the number of lattice sites, V. This is a general expression, previously derived by Helfand,[10] for the configurational entropy of long chains in the Markovian approximation. In the following section we will use this to treat the specific case of the semicrystalline interface.

In a better alternative approximation, we consider the conditional probabilities to be dependent on the location of the previous two segments. This permits elimination of those configurations which would turn back upon themselves immediately. We thus approximate the conditional probability by

$$p(\mathbf{r}_{k+1}|\mathbf{R}_k) = p(\mathbf{r}_{k+1}|\mathbf{r}_k,\mathbf{r}_{k-1}) \tag{16}$$

These factors need not be purely entropic; they can include Boltzmann factors to represent bending energies. We do not do so here, however; we consider only freely flexible chains. Substituting this into eq 7 and following the same procedure as before (eq 10–12)

$$S^{(2)} = k_B \sum_k \sum_{\substack{\mathbf{r}_{k+1},\mathbf{r}_k \\ \mathbf{r}_{k-1}}} p(\mathbf{r}_{k+1},\mathbf{r}_k,\mathbf{r}_{k-1}) \cdot \ln p(\mathbf{r}_{k+1}|\mathbf{r}_k,\mathbf{r}_{k-1}) - k_B \ln (\omega/\Psi) \quad (17)$$

The three-segment joint distribution is a product of factors

$$p(\mathbf{r}_{k+1},\mathbf{r}_k,\mathbf{r}_{k-1}) = p(\mathbf{r}_{k+1}|\mathbf{r}_k,\mathbf{r}_{k-1}) p(\mathbf{r}_k|\mathbf{r}_{k-1}) p(\mathbf{r}_{k-1}) \quad (18)$$

Substituting this into eq 17 and assuming the segments have no spatial preference, we obtain the two-segment approximation for the entropy

$$S^{(2)} = -k_B \sum_{\substack{\mathbf{r}_{k-1},\mathbf{r}_k \\ \mathbf{r}_{k+1}}} p(\mathbf{r}_{k+1}|\mathbf{r}_k,\mathbf{r}_{k-1}) p(\mathbf{r}_k|\mathbf{r}_{k-1}) \cdot \ln p(\mathbf{r}_{k+1}|\mathbf{r}_k,\mathbf{r}_{k-1}) - k_B \ln (\omega/\Psi) \quad (19)$$

where we have again ignored end effects. At this level of approximation knowledge of both the one-segment conditional and two-segment conditional probabilities are needed. We treat the semicrystalline interface in these two levels of approximation in the following section.

Semicrystalline Interface

One-Segment Conditional Probability. In the case of the semicrystalline polymer we assume the conditional probabilities depend only on the distance from the interface and are the same for all sites in a given layer. Consider the kth segment to be in a site in the lth layer. The conditional probability is zero for nonneighboring sites and is

$$\begin{aligned} p(\mathbf{r}_{k+1}|\mathbf{r}_k) &= p_l(+): \quad \mathbf{r}_{k+1} \text{ in } l+1 \\ p(\mathbf{r}_{k+1}|\mathbf{r}_k) &= p_l(0): \quad \mathbf{r}_{k+1} \text{ in } l \\ p(\mathbf{r}_{k+1}|\mathbf{r}_k) &= p_l(-): \quad \mathbf{r}_{k+1} \text{ in } l-1 \end{aligned} \quad (20)$$

for the neighboring sites. We substitute eq 20 int eq 15. The sum over $\mathbf{r}_k$ is replaced by $N_0 \sum_l$, and the sum over $\mathbf{r}_{k+1}$ represents all the sites accessible up, down, and sideways from a given position in layer l

$$S^{(1)} = -k_B N_0 \sum_l [p_l(+) \cdot \ln p_l(+) + (z-2) p_l(0) \cdot \ln p_l(0) + p_l(-) \cdot \ln p_l(-)] - k_B \ln (\omega/\Psi) \quad (21)$$

where N_0 is the number of sites in a layer. If there were no crystal constraints and the chain organization were completely amorphous, then

$$p(\mathbf{r}_{k+1}|\mathbf{r}_k) = 1/z \quad (22)$$

The presence of the crystal interface, however, imposes constraints in layers $l = 0$ and $l = M + 1$, which cause the conditional probabilities to differ from the bulk value. Those probabilities are determined by maximizing the entropy.

The conditional probabilities are not free to take on any values. For long chains, they are subject to two types of constraints. The first is that the conditional probabilities must be normalized

$$\sum_{\mathbf{r}_{k+1}} p(\mathbf{r}_{k+1}|\mathbf{r}_k) = 1 \quad (23)$$

This constraint is equivalent to what has previously been termed a conservation constraint[9] (see Appendix A); for the interphase it reduces to

$$p_l(+) + (z-2) p_l(0) + p_l(-) = 1 \quad (24)$$

The second constraint is due to the symmetry of the polymer configuration with respect to its two ends.[10,11] The probability for any configuration in one direction must be equal to the same configuration taken in the opposite direction along the chain. Thus

$$p(\mathbf{r}_{k+1},\mathbf{r}_k) = p(\mathbf{r}'_{k+1},\mathbf{r}'_k) \quad (25)$$

for

$$\mathbf{r}_k = \mathbf{r}'_{k+1} \quad \text{and} \quad \mathbf{r}_{k+1} = \mathbf{r}'_k \quad (26)$$

This constrains the conditional probabilities to satisfy

$$p_l(+) = p_{l+1}(-) \quad (27)$$

Because of these two constraints there is only one independent variable.

The entropy may be written in terms of only $p_l(-)$; for example

$$S^{(1)} = -k_B N_0 \sum_l [p_{l+1}(-) \ln p_{l+1}(-) + (1 - p_l(-) - p_{l+1}(-)) \cdot \ln (1 - p_l(-) - p_{l+1}(-))/(z-2) + p_l(-) \ln p_l(-)] - k_B \ln (\omega/\Psi) \quad (28)$$

$S^{(1)}$ can be maximized by differentiating with respect to $p_l(-)$. This yields the second-order difference equation

$$(z-2)^2 p_l^2(-) = [1 - p_l(-) - p_{l+1}(-)][1 - p_l(-) - p_{l-1}(-)] \quad (29)$$

which is subject to two boundary conditions. In the crystallite, there are no lateral steps. Thus at the two interfaces

$$p_0(-) = \tfrac{1}{2} \quad \text{and} \quad p_{M+2}(-) = \tfrac{1}{2} \quad (30)$$

where the factor one-half accounts for the two equivalent bond directions. This difference equation is equivalent to the one Helfand has previously used to study polymers at a wall.[11] The boundary conditions for the present case are different from those for the wall, however.

Two-Segment Conditional Probabilities. The two-segment conditional probabilities depend on the layer index of the three segments involved. For the kth segment in the lth layer there are nine possible conditional probabilities. Segments $k-1$ and $k+1$ may be in layers $l+1$, l, or $l-1$. For the neighboring sites of $\mathbf{r}_k$ they are given by the matrix

$$p(\mathbf{r}_{k+1}|\mathbf{r}_k,\mathbf{r}_{k-1}) = \begin{bmatrix} p_l(+|+) & p_l(+|0) & p_l(+|-) \\ p_l(0|+) & p_l(0|0) & p_l(0|-) \\ p_l(-|+) & p_l(-|0) & p_l(-|-) \end{bmatrix} \quad (31)$$

where $p_l(\alpha|\beta)$ is the two-segment conditional probability that segment $k+1$ is in layer $l + \alpha \cdot 1$ given that segment k is in layer l and segment $k-1$ is in layer $l + \beta \cdot 1$. α and β represent either +, 0, or −. We eliminate those configurations that immediately turn back upon themselves by setting

$$p_l(+|+) = p_l(-|-) = 0 \quad (32)$$

and also by the choice of the degeneracy factor for three-segment configurations within a single layer.

The entropy depends on both the two-segment and one-segment conditional probabilities. We substitute the layer-dependent probabilities into eq 19. Converting the $\mathbf{r}_k$ sum to a sum over l and carrying out the sums over the neighboring sites yields

$$S^{(2)} = -k_B N_0 \sum_l \{(z-2) p_l(+|0) p_l(0) \cdot \ln p_l(+|0) + p_l(+|-) p_{l-1}(+) \cdot \ln p_l(+|-) + (z-2) p_l(0|+) p_{l+1}(-) \cdot \ln p_l(0|+) + (z-2)(z-3) p_l(0|0) p_l(0) \cdot \ln p_l(0|0) + (z-2) p_l(0|-) p_{l-1}(+) \cdot \ln p_l(0|-) + p_l(-|+) p_{l+1}(-) \cdot \ln p_l(-|+) + (z-2) p_l(-|0) p_l(0) \cdot \ln p_l(-|0)\} - k_B \ln (\omega/\Psi) \quad (33)$$

There are again a number of constraints the probabilities must satisfy. The constraints on the one-segment conditional probabilities are still given by eq 24 and 27. The two constraints also apply to the two-segment conditional probabilities. Normalization requires

$$\sum_{\mathbf{r}_{k+1}} p(\mathbf{r}_{k+1}|\mathbf{r}_k,\mathbf{r}_{k-1}) = 1 \tag{34}$$

In terms of the layered indices this is

$$\begin{aligned} (z-2)p_l(0|+) + p_l(-|+) &= 1 \\ p_l(+|0) + (z-3)p_l(0|0) + p_l(-|0) &= 1 \\ p_l(+|-) + (z-2)p_l(0|-) &= 1 \end{aligned} \tag{35}$$

where we have used eq 32. The symmetry condition with respect to direction along the chain is equivalent to

$$p(\mathbf{r}_{k+1},\mathbf{r}_k,\mathbf{r}_{k-1}) = p(\mathbf{r}'_{k+1},\mathbf{r}_k,\mathbf{r}'_{k-1}) \tag{36}$$

for

$$\mathbf{r}_{k+1} = \mathbf{r}'_{k-1} \quad \text{and} \quad \mathbf{r}_{k-1} = \mathbf{r}'_{k+1} \tag{37}$$

The three-segment joint probability can be written in terms of the one- and two-segment conditional probabilities. For the kth segment in the lth layer it is given by the matrix

$$Vp(\mathbf{r}_{k+1},\mathbf{r}_k,\mathbf{r}_{k-1}) = \begin{bmatrix} 0 & p_l(+|0)p_l(0) & p_l(+|-)p_{l-1}(+) \\ p_l(0|+)p_{l-1}(-) & p_l(0|0)p_l(0) & p_l(0|-)p_{l-1}(+) \\ p_l(-|+)p_{l+1}(-) & p_l(-|0)p_l(0) & 0 \end{bmatrix} \tag{38}$$

where the ordering is the same as in the conditional probability matrix. The symmetry constraint requires the joint probability matrix to be symmetric about its diagonal and thus

$$\begin{aligned} p_l(+|0)p_l(0) &= p_l(0|+)p_{l+1}(-) \\ p_l(+|-)p_{l-1}(+) &= p_l(-|+)p_{l+1}(-) \\ p_l(0|-)p_{l-1}(+) &= p_l(-|0)p_l(0) \end{aligned} \tag{39}$$

must be satisfied. These six constraint equations reduce the number of independent two-segment conditional probabilities to one. These constraint equations have previously been called the continuity constraint[9] (see Appendix A).

In a bulk amorphous system the two-segment conditional probabilities are

$$p(\mathbf{r}_{k+1}|\mathbf{r}_{k-1}) = 1/(z-1) \tag{40}$$

for all sites and the one-segment conditional probabilities are $1/z$. These values satisfy the six constraint equations above and those for the one-segment conditional probabilities. To determine the probabilities for the semicrystalline interphase we maximize the entropy (eq 33) subject to the constraints and the boundary conditions

$$p_0(-) = \tfrac{1}{2} \qquad p_0(+|0) = 0 \qquad p_0(-|0) = 1 \tag{41}$$

and

$$p_{M+2}(-) = \tfrac{1}{2} \qquad p_{M+1}(-|0) = 0 \qquad p_{M+1}(+|0) = 1 \tag{42}$$

The eight constraints reduce the number of independent variables to one one-segment conditional probability and one two-segment conditional probability. Maximization of the entropy yields a set of difference equations. The difference equations are most easily obtained by a direct reduction of the number of variables followed by maximization with respect to the remaining variables. The rather lengthy algebra is straightforward and yields a set of equations which are solved numerically. The results are given in the following section.

Table I
One-Segment Approximation: Conditional Probabilities and Order Parameter[a]

layer (l)	$p_l(-)$	$(z-2)p_l(0)$	s_l
0	$^1/_2$	0.3722	0.4417
1	0.1278	0.7017	−0.0525
2	0.1705	0.6632	0.0005
3	0.1663	0.6670	0.0001
4	$^1/_6$	$^2/_3$	0

[a] Calculations are for a cubic lattice, $z = 6$.

Table II
Two-Segment Approximation: Conditional Probabilities and Order Parameter[a]

layer (l)		$p_l(-)$	$p_l(+\|0)$	$p_l(-\|0)$	s_l
0	$^1/_2$	0.3663	0	1	0.4504
1	0.1337	0.6963	0.2066	0.1545	−0.0445
2	0.1700	0.6637	0.1993	0.2048	0.0045
3	0.1663	0.6670	0.2001	0.1995	−0.0005
4	$^1/_6$	$^2/_3$	$^1/_5$	$^1/_5$	0

[a] Calculations are for a cubic lattice, $z = 6$.

Results

The difference equations which result from maximation of the entropies are solved as a set of simultaneous equations for a fixed number of amorphous layers ($M + 1$). The results are independent of M for $M > 11$.

In Tables I and II we report the values of the conditional probabilities for the two levels of approximation considered here. The other probabilities can easily be constructed by using the appropriate constraint equations. By symmetry the conditional probabilities at the opposite crystalline face are equivalent, but $p_l(+|0)$ and $p_l(-|0)$ reverse roles. By layer $l = 4$ the configurational anisotropy has vanished and the conditional probabilities take on their random values.

The order parameter in each layer is

$$s_l = 1 - \tfrac{3}{2}\langle \sin^2 \theta \rangle_l \tag{43}$$

where θ is the angle between a bond and the normal to the crystal face. It can be expressed as

$$s_l = 1 - 3(z-2)p_l(0)/2 \tag{44}$$

for the cubic lattice.

Predicted values for the order parameter are shown in Figure 2. The two levels of approximation are indistinguishable on that scale. Results of the Flory, Yoon, and Dill (FYD) calculation are also shown for the freely flexible chain ($\eta = 1$).[9] The present calculations predict a sharper interphase than that of the FYD treatment. The present treatment also predicts a much higher incidence of tight folds in the zeroth layer than the earlier treatment. It is predicted that 74.4% of the chains from the crystal are adjacent reentrants in the one-segment approximation; 73.3% in the two-segment approximation. This may be compared to 72% in the Monte Carlo simulation,[8] 42% in the FYD model,[9] and $^2/_3$ predicted by random statistics.[7] Other conformational properties may be computed from the values in Tables I and II; they all predict a narrower interface than in the FYD treatment. These differences can be attributed to a poor approximation in the partition function in the FYD treatment. In that work the partition function is taken to be the product of two independent factors, one due to the distribution of vertical and horizontal bonds, and the other due to the distribution of orientations of segments connecting the vertical bonds. The vertical bonds are enumerated in the conditional probabilities of the latter factor and in the unconditional probabilities in the former factor. The overcounting of vertical bonds leads to an underestimate for the partition

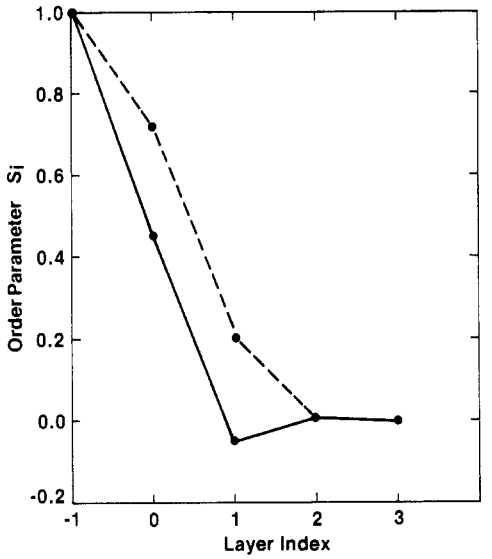

Figure 2. Bond orientational order parameter as a function of distance from the crystal boundary. The solid line is from the results obtained by maximizing the configurational entropy (eq 28 or eq 33). The dashed line is the freely flexible result (η = 1) of FYD.

function and an underestimate for the configurational freedom of the chains.

Although the interfacial zone is small, its effect on the chains that extend into the amorphous region is not. The relative proportion and mean lengths of the amorphous loops and ties is significantly altered. Previously Guttman, DiMarzio, and Hoffman[7] modeled the chain configurations between crystallite surfaces of semicrystalline polymers as random walks with absorbing boundary conditions at the two crystalline faces. We show below that the interfacial constraints, however, lead to significantly different mean lengths and numbers of loops and ties than that predicted by random statistics. To do so we solve the gambler's ruin problem[7,13] with variable step probabilities specified by the present interphase theory.

Consider the probability, L_n, that a walk starts at layer $l = n$ and ends at $l = 0$. The probability that an amorphous configuration is a loop is L_1 while the probability it is a tie configuration is L_M. L_n obeys the difference equation[13]

$$L_n = p_{n+1}(-)L_{n+1} + (z-2)p_n(0)L_n + p_{n-1}(+)L_{n-1} \quad (45)$$

with the boundary conditions

$$L_0 = 1 \quad \text{and} \quad L_{m+1} = 0 \quad (46)$$

For random walks the one-segment conditional probabilities are $1/z$ and

$$L_n = 1 - n/(M+1) \quad (47)$$

Thus if the step probabilities were those of a purely amorphous system up to the crystal boundary, the probability of a loop configuration would be $M/(M+1)$ and that of a tie configuration $1/(M+1)$. We would thus expect the ratio of the number of amorphous loops to tie configurations to be equal to M, the width of the amorphous region. The interfacial constraints alter the one-step probabilities, however. We have numerically solved the difference equation, eq 45, for L_n using the values of the one-segment conditional probabilities listed in Tables I and II for amorphous regions varying from $M + 1 = 12$ to $M + 1 = 45$. In Table III we list the ratios of the loop to tie probabilities divided by M. Results for $M + 1 = 12$, 20, and 45 are given for both the one-segment and two-segment approximations. These should be compared to the

Table III
Ratio of Amorphous Loops to Ties[a]

	$(L_1/L_M)/M$	
$M+1$	1-segment approx	2-segment approx
12	0.785	0.817
20	0.777	0.812
45	0.771	0.806

[a] L_1 is the probability of an amorphous loop and L_M is the probability of an amorphous tie.

Table IV
Mean Length of Amorphous Walks[a]

	$(D_1+1)/(M+1)$	
$M+1$	1-segment approx	2-segment approx
12	3.67	3.51
20	3.77	3.60
45	3.85	3.68

[a] $D_1 + 1$ is the mean length of an amorphous walk.

values of unity for random walks and the value of $\approx 1/2$ found by Mansfield[8] by Monte Carlo simulations. The results in Table III from the two levels of approximation are qualitatively the same. The interfacial constraints decrease the number of loop configurations relative to the random walk approximation but loops are still more numerous than tie configurations by an order of the width of the amorphous zone. Mansfield obtained an even greater decrease of loops relative to the random walk approximation.

The mean lengths of all amorphous walks (i.e., loops and ties) can be calculated by considering D_n, the expected duration of a walk that starts at $l = n$ and terminates if it reaches either $l = 0$ or $M + 1$. D_n satisfies the difference equation[13]

$$D_n = p_{n+1}(-)D_{n+1} + (z-2)p_n(0)D_n + p_{n-1}(+)D_{n-1} + 1 \quad (48)$$

subject to the boundary conditions

$$D_0 = 0 \quad \text{and} \quad D_{M+1} = 0 \quad (49)$$

The mean length of an amorphous walk is given by $D_1 + 1$, where the factor of one accounts for the initial step from layer $l = 0$ into the amorphous region. For random walks on a cubic lattice ($z = 6$)

$$D_n = 3n^2 + 3n(M+1) \quad (50)$$

and the mean length, $D_1 + 1$, is $3M + 1$. The results from numerically solving eq 48 using the probabilities for the constrained walks are given in Table IV. We list the results for $M + 1 = 12$, 20, and 45 from the two different approximations. We find that the effect of the constraints is to increase the average length of an amorphous walk relative to the random walk. The dependence on the width of the amorphous zone is predicted to be unchanged, however. This agrees with Mansfield's Monte Carlo results; he finds that the average amorphous walk has a length of $\approx 3.5\ (M + 1)$.

The mean lengths of the two types of amorphous walks, loops and ties, can be obtained by considering $u_{n,i}$, the probability that a walk reaches $l = 0$ at the ith step given that it starts at $l = n$. It satisfies the difference equation[13]

$$u_{n,i+1} = p_{n+1}(-)u_{n+1,i} + (z-2)p_n(0)u_{n,i} + p_{n-1}(+)u_{n-1,i} \quad (51)$$

subject to the boundary conditions

$$u_{0,i} = u_{M+1,i} = 0: \qquad i \geq 1 \quad (52)$$

and

$$u_{0,0} = 1, \qquad u_{n,0} = 0: \qquad n > 0 \quad (53)$$

Table V
Mean Lengths of Amorphous Loops and Ties

	1-segment approx		2-segment approx	
$M+1$	$\langle loop\rangle/(M+1)$	$\langle tie\rangle/(M+1)^2$	$\langle loop\rangle/(M+1)$	$\langle tie\rangle/(M+1)^2$
12	2.59	1.08	2.48	1.07
20	2.60	1.05	2.48	1.04
45	2.60	1.02	2.49	1.02

The mean length of an amorphous loop, $\langle loop\rangle$, is given by

$$\langle loop\rangle = 1 + \sum_{i=0}^{\infty} iu_{1,i} / \sum_{i=0}^{\infty} u_{1,i} \tag{54}$$

and for an amorphous tie

$$\langle tie\rangle = 1 + \sum_{i=0}^{\infty} iu_{M,i} / \sum_{i=0}^{\infty} u_{M,i} \tag{55}$$

Rather than solve for the full probability, $u_{n,i}$, we rewrite the mean loop and tie lengths in terms of

$$\mu_n = \sum_{i=0}^{\infty} iu_{n,i} \tag{56}$$

and

$$L_n = \sum_{i=0}^{\infty} u_{n,i} \tag{57}$$

where L_n is given by eq 45. An equation for μ_n is obtained by multiplying eq 51 by i and summing

$$\mu_n = p_{n-1}(+)\mu_{n-1} + p_{n+1}(-)\mu_{n+1} + (z-2)p_n(0)\mu_n + L_n \tag{58}$$

which is subject to the boundary conditions

$$\mu_0 = 0 \quad \text{and} \quad \mu_{M+1} = 0 \tag{59}$$

For random walks L_n is given by eq 47 and for a cubic lattice

$$\mu_n = 2(M+1)n - 3n^2 + n^2/(M+1) \tag{60}$$

Thus if the amorphous region were random, then

$$\langle loop\rangle_{random} = 2(M+1) \tag{61}$$

and

$$\langle tie\rangle_{random} = (M+1)^2 \tag{62}$$

In Table V we list the mean lengths for loops and ties for $M+1 = 12$, 20, and 45 obtained by numerically solving eq 58 and 45 using the nonrandom step probabilities listed in Tables I and II. We find the interphase constraints do not affect the dependence on the width of the amorphous region of the amorphous loops or ties but that they increase the mean length of amorphous loops. This can be compared to the Monte Carlo results of Mansfield

$$\langle loop\rangle_{Monte\ Carlo} \approx 2.4(M+1) \tag{63}$$

and

$$\langle tie\rangle_{Monte\ Carlo} \approx 0.6(M+1)^2 \tag{64}$$

The average loop length is in reasonable agreement with the Monte Carlo results but our prediction for the mean length of tie configurations is significantly larger. It is possible that the differences of the present treatment and the Monte Carlo simulations are due to the nonergodicity of the latter. It is likely that the frequency and length of the tie configurations would be most sensitive to sampling errors due to their relative infrequency.

The models presented here for predicting the chain conformations in the semicrystalline interphase are subject to two limitations. First, we have treated only the conformational equilibrium; we have made no attempt to account for effects of kinetic constraints. For circumstances in which entanglements of long chains may reach equilibrium more slowly than experimental conditions permit, kinetics may significantly affect the observed chain conformations. For example, the interphase is likely to be broadened due to a decrease in the number of configurational states which are accessible over short times. Second, we have neglected bending energies of the chains and any additional energies that may be associated with the tight hairpin bends required to permit suitable packing in the crystal. Thus while the models of freely flexible chains considered here predict a high incidence of hairpin loops, the incidence in real systems is likely to be smaller. Thus the value of the present model is not in its prediction of the fractional adjacency of reentry for real systems, but in its predictions for a useful reference state, that of the freely flexible chain, and in providing a systematic treatment for different levels of approximation into which such bending energies can be readily incorporated.

Acknowledgment. We thank Dr. Clayton Henderson for detailed reading of the manuscript and many helpful suggestions and the NIH for grant support.

Appendix A

In this appendix, we show that the constraint equations used by Flory, Yoon, and Dill[9] (FYD) derive in a simple way from the present conditional probability normalization conditions. For the purpose of this comparison, we consider only chains with no inherent bending energies (i.e., the FYD parameter $h = 1$).

The elementary unit in the FYD treatment is a bond, composed of two connected segments; the elementary unit in the present treatment is the individual segment. We identify

$$\begin{aligned} p_l(+) &= p_{l+1}/2 \\ p_l(0) &= q_l/(z-2) \\ p_l(-) &= p_l/2 \end{aligned} \tag{A.1}$$

On the left-hand side are the one-segment conditional probabilities defined in eq 20 in the text. On the right-hand side are the bond orientation probabilities of FYD; i.e., p_l is the number of bonds between layers l and $l-1$ divided by the number of sites, and q_l is the number of bonds in layer l divided by the number of sites. The factors of two which divide these probabilities are due to the indistinguishability of direction of a vertical bond. The factor of $(z-2)$ is due to the indistinguishability of direction of a horizontal bond. These factors arise because in the present treatment, each site is considered distinguishable, whereas in FYD any lateral bond, for example, is considered indistinguishable from any other. This difference is of little importance other than for purposes of making the present comparison.

The FYD constraint that the lattice be fully filled (the conservation constraint) is

$$q_l + p_{l+1}/2 + p_l/2 = 1 \tag{A.2}$$

Using eq A.1, one clearly sees that the FYD constraint condition eq A.2 is identical with the normalization condition for the one-segment conditional probabilities, eq 24.

Next we consider the two-segment conditional probabilities, i.e., for the conformation of bond-pair junctions:

$$p_l(+|0) = u_{l+}$$
$$p_l(0|0) = u_{l0}/(z-3) \quad \text{(A.3)}$$
$$p_l(-|0) = u_{l-}$$

The two-segment conditional probabilities on the left are defined by eq 31. The terms on the right are defined by FYD as the statistical weights for bonds which are connected to horizontal bonds in layer l. The factor $(z-3)$ is due to indistinguishability of horizontal bond directions. Symmetry conditions, eq 39, permit the other two-segment conditional probabilities defined in eq 31 to be defined in terms of the quantities in eq A.3:

$$p_l(0|+) = u_{l+}p_l(0)/p_{l+1}(-)$$
$$p_l(0|-) = u_{l-}p_l(0)/p_l(-) \quad \text{(A.4)}$$

where we have used eq 27 to eliminate $p_{l-1}(+)$. The remaining two conditionals can be constructed by using two of the normalization constraints

$$p_l(-|+) = 1 - (z-2)u_{l+}p_l(0)/p_{l+1}(-)$$
$$p_l(+|-) = 1 - (z-2)u_{l-}p_l(0)/p_l(-) \quad \text{(A.5)}$$

The third normalization condition

$$u_{l+} + u_{l0} + u_{l-} = 1 \quad \text{(A.6)}$$

is common to the FYD and present treatment. One additional symmetry condition must be satisfied

$$p_l(-|+)p_{l+1}(-) = p_l(+|-)p_{l-1}(+) \quad \text{(A.7)}$$

Combination of these results leads to the continuity constraint of FYD (for $h = 1$)

$$p_{l+1}/2 - p_{l-}/2 = q_l(u_{l+} - u_{l-}) \quad \text{(A.8)}$$

Thus the constraint conditions of FYD are seen to follow from the symmetry and normalization conditions used in the present treatment. The partition functions differ, however; the consequences are described in the text.

References and Notes

(1) Mandelkern, L. *Faraday Discuss. Chem. Soc.* **1979**, *68*, 310.
(2) Flory, P. J. *J. Am. Chem. Soc.* **1962**, *84*, 2857.
(3) Peterlin, A. *Macromolecules* **1980**, *13*, 777.
(4) *Faraday Discuss. Chem. Soc.* **1979**, 68.
(5) DiMarzio, E. A.; Guttman, C. M. *Polymer* **1980**, *21*, 733.
(6) DiMarzio, E. A.; Guttman, C. M.; Hoffman, J. D. *Polymer* **1980**, *21*, 1379.
(7) Guttman, C. M.; DiMarzio, E. A.; Hoffman, J. D. *Polymer* **1981**, *22*, 1466.
(8) Mansfield, M. L. *Macromolecules* **1983**, *16*, 914.
(9) Flory, P. J.; Yoon, D. Y.; Dill, K. A. *Macromolecules* **1984**, *17*, 862.
(10) Helfand, E. *J. Chem. Phys.* **1975**, *63*, 2192.
(11) Helfand, E. *Macromolecules* **1976**, *9*, 307.
(12) Mullins, W. W. *Phys. Rev.*, **1959**, *114*, 389.
(13) Feller, W. *An Introduction to Probability Theory and Its Applications*; Wiley: New York, 1968; Vol. I.

Molecular Relaxations in Halar, an Alternating Copolymer of Ethylene and Chlorotrifluoroethylene

Yash P. Khanna* and John P. Sibilia

Corporate Technology, Allied Corporation, Morristown, New Jersey 07960

Swayambu Chandrasekaran

Plastics and Engineering Materials Division, Chemical Sector, Morristown, New Jersey 07960.

Received February 17, 1986

ABSTRACT: Molecular relaxations in Halar, a predominantly alternating 1:1 copolymer of ethylene (E) and chlorotrifluoroethylene (CTFE), have been studied with dynamic mechanical analysis as the primary technique. The mechanisms of the four relaxations, α, β', β'', and γ, occurring over the −130 to +230 °C region have been studied by changing physicochemical variables such as crystallinity, molecular weight, and the degree of alternation. The α-relaxation occurs between +100 and +200 °C and is determined primarily by the crystalline characteristics, i.e., crystallinity, crystallite thickness, and/or crystallite perfection. Motions of the polymer segments at the crystalline–amorphous interface, characterized by a very high activation energy of 129 kcal/mol, are believed to be responsible for the α-relaxation. The onset of the β'-relaxation at 65 °C is identified as the glass transition (T_g) of Halar. The β'-peak occurs at about 85 °C. The β''-relaxation at 50 °C is also an amorphous phenomenon but is believed to involve shorter segments than those responsible for the β'-relaxation or the T_g. A lower activation energy of the β''-process relative to that of the β'-process (66 vs. 107 kcal/mol) supports this assignment. The γ-relaxation occurs at about −55 °C but extends from −120 to +20 °C. Our results suggest that small units of the polymer chain, perhaps 3–4 carbon atoms in length, belonging to various physicochemical environments may be responsible for the γ-peak. Its activation energy, i.e., 27 kcal/mol, is also the lowest of all the relaxations in Halar.

Introduction

Halar is the trademark for Allied Corporation's copolymer products made from ethylene (E) and chlorotrifluoroethylene (CTFE). At present the major application of standard Halar (50E:50CTFE, alternating copolymer) is in the cable-coating industry where this material could be exposed to high temperatures. Accordingly, in a recent study we described the effect of high-temperature aging on the physicochemical characteristics of Halar, including a detailed analysis of the melting behavior.[1,2] Prior to melting, several molecular relaxations occur in polymers at characteristic temperatures which dictate the product applicability. Earlier we had reported a study of these molecular relaxations[3] in Halar in the −100 to +200 °C region based on mechanical spectra. Since then we have learned more about the phenomenon of molecular motions in Halar over the temperature range −130 to +230 °C, and this is the subject of the present paper.

Experimental Section

Materials. The samples selected for this study are listed in Table I. Halar 300 and Halar 500 differ only in molecular weight

0024-9297/86/2219-2426$01.50/0